Nanog promotes stem-like traits of glioblastoma cells

Yuan Ye[1], Mengsi Zhang[1], Guangning Yan[2], Qinghua Ma[1], Zexuan Yan[1],Lihong Wang[1], Kaidi Yang[1] , Deyu Guo[1]

[1]Institute of Pathology and Southwest Cancer Center, Southwest Hospital, Third Military Medical University (Army Medical University), and Key Laboratory of Tumor Immunopathology, Military of Education of China, Chongqing, China, [2]Department of Pathology, General hospital of southern theatre command, People's Liberation Army, Guangzhou, China

TABLE OF CONTENTS

1. ABSTRACT

Glioblastoma multiforme (GBM) is a highly aggressive brain tumor with poor progrnosis and a high recurrence rate after surgery. To this end, we examined the role of Nanog that is highly expressed in this tumor. *NANOG* is a transcription factor involved in the pluripotency of embryonic stem cells (ESCs) and the induction of malignancy in cancer stem-like cells (CSCs). Bioinformatic analysis revealed that *NANOG* may be associated with the development of stem-like traits in GBM. Forced expression of *NANOG* markedly increased the expression of cancer stem cell markers and

promoted the sphere formation and migration of GBM cells. Nanog enhanced the expression of SHH which is required for the maintenance of the positive feedback loop of Hedgehog signaling pathway. Treatment of GBM cells with SANT-1 and GANT61 significantly reduced the tumor progression. These data support a view that reduction of Nanog might have therapeutic benefits in GBM.

2. INTRODUCTION

Glioblastoma (GBM) is the most common and aggressive primary brain tumor in humans, with a current median survival of approximately 14 months (1). GBM displays remarkable cellular heterogeneity and hierarchy for containing glioma stem cells (GSCs) with potent tumorigenic capacity. GSCs are functionally defined by extensive self-renewal, multi-lineage differentiation, and potential to drive malignant growth *in vivo* (2). GSCs promote tumor angiogenesis, immune evasion, and recruitment of tumor-supportive macrophages to facilitate malignant growth, invasion and therapeutic resistance, thus, targeting GSCs is an important strategy for the treatment of GBM (3, 4).

Nanog is a core transcription factor, that encompasses a DNA-binding domain, and is part of the core regulatory network that suppresses differentiation and maintains pluripotency (5). Although, Nanog expression lacks prognostic value in rectal cancer, its expression is used as a biomarker that predicts a poor clinical outcome in oral squamous cell carcinoma (6, 7). Furthermore, Nanog expression closely relates with stem-like traits in some malignant cancers (8-10). To this end, we examined the effects of Nanog on stem cell-like properties and malignant biological behavior of GBM cells. Furthermore, we examined the positive feedback loop between Nanog and Hedgehog signaling pathway. We also show that up-regulation of Nanog enhances Shh-Gli-Nanog-Smo signaling network. *In vitro* and *in vivo* experiments demonstrate that combination of SANT-1 and GANT61 can significantly inhibit GBM progression. Collectively, this work provides a novel potential therapeutic target for the treatment of GBM.

3. MATERIALS AND METHODS

3.1. Cell culture and database

The human GBM cell line LN229 was purchased from ATCC (Manassas, VA). Primary GBM2 cells used in this study were derived from the GBM tumor tissues (Southwest Hospital, TMMU, China) and cultured as previously described (11). The cells were routinely cultured in DMEM medium containing 10% FBS, and maintained in presence of 5% CO_2 at 37^0 C. 284 patient specimens from Gravendeel_GBM database was utilized to evaluate the correlation between the expression of *NANOG*, and GLI1 and SMO. Non-targeting control vector lentivirus purchased from HanBio Technology Co. (Shanghai, China)

3.2. Microarray and data analysis

The microarray data of mRNA from 70 glioblastoma patient samples were downloaded from the NCBI's (Gene Expression Omnibus (GEO): GSE53733. These data were then separated into low and high group at the cut-off value of median expression of *NANOG*. Kyoto Encyclopedia of Genes and Genomes (KEGG) pathway analysis of this microarray was performed using KEGG Pathway Finder with a gene correlation that was based on *NANOG* expression using the R2 web application. Absolute r cutoff was equal to 0.5, P<0.05. Gene Set Enrichment Analysis (GSEA; http://www.broadinstitute.-org/gsea/index.jsp) was carried out using the Cell Adhesion Molecules CAMS, Cell Cycle and Apoptosis gene set and Gene Ontology (GO) Anchoring Junction gene set.

3.3. Lentivirus production and transduction

LN229 and GBM2 cells were seeded in 6-well plates at 2×10^5 cells/well in DMEM supplemented with 10% FBS. When cultures were approximately 60%-70% confluent, the medium was changed to 900 μL serum-free DMEM. The diluted OE *NANOG* and non-targeting control vector lentivirus was added to each well and dishes were incubated for 24 h. The medium was then changed, and then the samples were

Table 1. Primers used for qRT-PCR analyses in this study

Gene	Forward primer (5' to 3')	Reverse primer (5' to 3')
β-actin	GTACGACCAGAGGCATACAGG	GATGACGATATCGCTGCGCTG
SOX2	GCCGAGTGGAAACTTTTGTCG	GGCAGCGTGTACTTATCCTTCT
NANOG	TTTGTGGGCCTGAAGAAAACT	AGGGCTGTCCTGAATAAGCAG
OCT4	CTGGGTTGATCCTCGGACCT	CCATCGGAGTTGCTCTCCA
OLIG2	CCAGAGCCCGATGACCTTTTT	CACTGCCTCCTAGCTTGTCC
GLI1	GTGCCGTTTGGTCACATGG	AACGCTATACAGATCCTAGCTCG
GLI2	GCATGGAATGGTGGCAAGAG	CTGCCTCCGAGAAGCAAGAAG
SMO	GCAGGGTAGCGATTCGAGTT	GAAGTGCCCTTGGTTCGGA

incubated for 48 h. Puromycin-containing medium was then applied to select transduced cells.

3.4. Western blotting

Western blot assay was conducted as previously described (12, 13). In brief, proteins were separated using 8% SDS Tris-glycine gels and transferred onto a polyvinylidene difluoride membrane. Membranes were blocked with 5% fat-free milk and incubated with antibodies against β-actin (Beyotime Institute of Biotechnology, Beijing, China), Nanog, Sox2, Oct4, CD133, Gli1, Gli2, Smo (Cell Signaling Technology, Beverly, MA) overnight at 4℃. Then, an appropriate secondary antibody (anti-mouse or anti-rabbit IgG; Beyotime Institute of Biotechnology, Beijing, China) was applied on the membranes. Immunoreactivity was detected using an ECL Kit (Pierce, Thermofisher, Chino CA). The results were analyzed using Image Lab Software (Bio-Rad Laboratories).

3.5. qRT-PCR analysis

Total RNA from cultured cells was extracted using RaPure Total RNA Mini Kit (Magen) according to the manufacturer's protocol. qRT-PCR was carried out using the 5×PrimeScript RT Master Mix (TaKaRa). All reactions were performed in a C1000TM Thermal cycler (Bio-Rad CFX96TM Real-time System). The results from qRT-PCR were normalized using the threshold cycle of β-actin. Targeted genes were amplified with primers listed in Table 1. The total volume of each reaction was 10 μL, and the relative expression of the target gene was analyzed by the comparative cycle threshold ($2^{-\Delta\Delta Ct}$) method.

3.6. Limiting dilution analysis

GBM cells were harvested and seeded into 96-well plates at a density of 5, 10, 20 cells/well with 10 replicates. Fourteen days after implantation, the efficiency of sphere formation was calculated using extreme limiting dilution analysis as described (14).

3.7. Plate clone formation assay

Two hundred cells were into 6-well plates and cultured for 14 days. After washing with phosphate-buffered saline (PBS), cells were fixed with 20% methanol for 15 min. Then, Giemsa solution was added to each dish for 5 min. After washing and air drying, clones were counted using a cloning counter. A total of 100 clones was counted in each dish. Rate of formation of clones was assessed by the following formula.

Rate of clone formation (%) = (number of clones/number of inoculated cells) × 100%.

3.8. Transwell migration assay

Dishes were trypsinized and the total number of cells was counted. Then, 1×10^4 cells and serum-free cell culture medium (200 μL) were added to each cell culture insert (8.0 μm; Millipore). In each well of 24 well culture dishes, 500 μL medium with 10% FBS was added and then inserts were inserted to each well and the dishes were placed at 37℃. After 24 h of incubation, the inserts were washed with

Table 2. The plasmid sequences used in luciferase assay

Gene	Forward primer (5' to 3')	Reverse primer (5' to 3')
Vector	TTTGGGAAGCCGAGGTG	TGCGATCTTGGCTCACT
OE *NANOG*	CCCTGCCTCAGCCTCGGAAAGT	CCCTGCCTCAGCCTCGGAAAGT
SMO Promoter	AGGTTGCAGTGAGCCAAGA	AAGCCTAGCCCAGCAGAGCC
pGL4-luc2 Vector	TGGGCTAGGCTTCGTTG	AGGACCTCAGCAGGAAAA
pRL-TK Vector	AGGTCCTGGAATACTAAAGGG	TAAATGCCGCCATCTGC

phosphate-buffered saline (PBS) and fixed for 15 minutes in 4% paraformaldehyde. The cells on the top of each insert were removed and then the inserts were stained by crystal violet solution (Beyotime Institute of Biotechnology, Beijing, China). A total number of 200 cells were counted under a microscope.

3.9. Luciferase assay

GBM cells were plated in 24- well plates for 24 h before being transfected with pGL4-luc2 vector encompassing the SMO promoter or control Renilla luciferase plasmid (pRL-TK). After 24h of incubation, cells were transfected with *NANOG* expression vector or the corresponding empty vector (GENECHEM, Shanghai, China). The experimental plasmid to control plasmid ratio was 50:1. Luciferase assays were performed with the Dual Luciferase Reporter Assay System (Promega). Briefly, 24-48 h post-transfection, cell lysates were prepared by incubating the cells with 1× passive lysis buffer for 15 min at room temperature. Cell lysates were transferred in triplicates to 96-well plates and analyzed on a Varioskan Flash Luminometer (Thermo Scientific) according to the manufacturer's instruction. The firefly luminescence signal was normalized to the Renilla luminescence signal. The sequences of luciferase plasmids are listed in Table 2.

3.10. CCK-8 assay

2×10^3 LN229 and GBM2 cells were sorted by FACS and seeded in 96-well cell culture plates in six replicates in 100 µL medium with 10% serum overnight. Cells were divided into four groups; the control group received DMSO, the S group received 20 nM SANT-1, the G group received 5 µM GANT61 and the S+G group received 20 nM SANT-1 and 5 µM GANT61.

NANOG overexpressing cells, corresponding control and WT (wild type) LN229 and GBM2 cells that were sorted by FACS were seeded at 2×10^3 cells/well in 96-well plates with six replicates. Viability of cells was assessed by production of CCK-8 formazan (C0038, Beyotime) for 7 days and the OD-values were recorded by fluoroanalyzer (Floskan Ascent) at OD of 450 nm.

3.11. Xenograft in NOD-SCID mice

The animal study was performed in accordance with the protocol approved by the Institutional Animal Care and Use Committee of Southwest Hospital, Third Military Medical University (TMMU). Five week-old NOD/SCID female mice were purchased from Laboratory Animal Center of TMMU. LN229 cells were divided into four groups; the control group received DMSO, the S group received 20 nM SANT-1, the G group received 5 µM GANT61 and the S+G group received 20 nM SANT-1 and 5 µM GANT61.

All groups of GBM cells were pre-treated with SANT-1, GANT61 or SANT-1 and GANT61 for three days. Then four groups of GBM cells were washed and re-suspended in PBS and mixed with Matrigel (1:1, BD Biosciences). 4×10^5 cells in 100 µL matrigels were injected subcutaneously into right back of NOD/SCID mice. After 25 days, mice were sacrificed, and the tumors were removed and their weight were measured.

3.12. Statistical analysis

Results were obtained from at least three experiments. Data are expressed as the mean ±SD by comparing the experimental and control groups using SPSS 16.0 statistical software (SPSS Inc.,
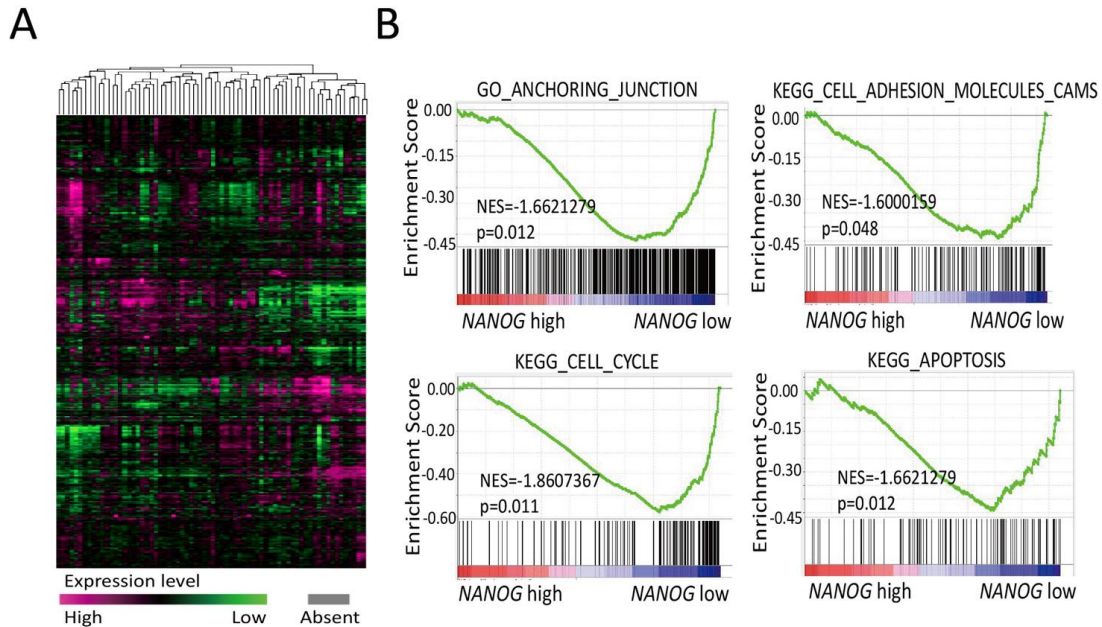
Figure 1. *NANOG* is associated with stem-like traits of GBM cells evaluated by GSEA enrichment analysis. (A) Heat map of expression values for differentially expressed genes from 70 glioblastoma patients were obtained from the GEO database (GSE53733). (B) GSE53733 data set was analyzed with GSEA enrichment plots of the GO Anchoring Junction gene set, KEGG Cell Adhesion Molecules Cams, Cell Cycle and Apoptosis. GBM, glioblastoma; GEO, Gene Expression Omnibus; GO, Gene Ontology; GSEA, Gene Set Enrichment Analysis; KEGG, Kyoto Encyclopedia of Genes and Genomes.

Chicago, IL, USA). When two groups were compared, the unpaired Student's t-test or by two-way ANOVA test was used. Multiple comparisons between the groups was performed using S-N-K method. Data are presented as the mean ±SD. Statistical significance was set at *** P < 0.001, ** P < 0.01, * P < 0.05.

4. RESULTS

4.1. *NANOG* expression in GBM

In order to illustrate the role of *NANOG* in GBM cells, microarray of 70 GBM patient samples (GSE5373) were obtained from GEO database (Figure 1A). GSEA analysis showed that *NANOG* expression negatively correlated with the expression of genes which are responsible for anchoring junction, cell cycle, apoptosis, and cell adhesion in the context of GO_ANCHORING_JUNCTION,-KEGG_CELL_ADHESION_MOLECULES,KEGG_C ELL_CYCL,KEGG_APOPTOSIS gene-set. Such negative correlation suggest that *NANOG* might

impact cell division, migration, and apoptosis (Figure 1B).

4.2. Establishing *NANOG* overexpression (OE) GBM cells

Nanog has been reported to regulate "stemness" in some malignant tumors. To decipher the role of *NANOG* in GBM, LN229 and GBM2 cells were transduced with *NANOG*-OE lentivirus. Flow cytometry and microscopic examination for florescence protein (GFP) showed that over 90% of cells were GFP-positive (Figure 2A-B). qRT-PCR and Western blot assays showed that the expression of Nanog was significantly increased in *NANOG*-OE LN229 and GBM2 cells as compared with the cells that were transduced with empty vector (Figure 2C). To determine whether overexpression of *NANOG* into the GBM cells impacts the number of cancer stem cells, we assessed the CD133, OCT4 and SOX2 in the transduced cells by qRT-PCR and Western blot assays. These analyses showed that the expression of all three genes was markedly
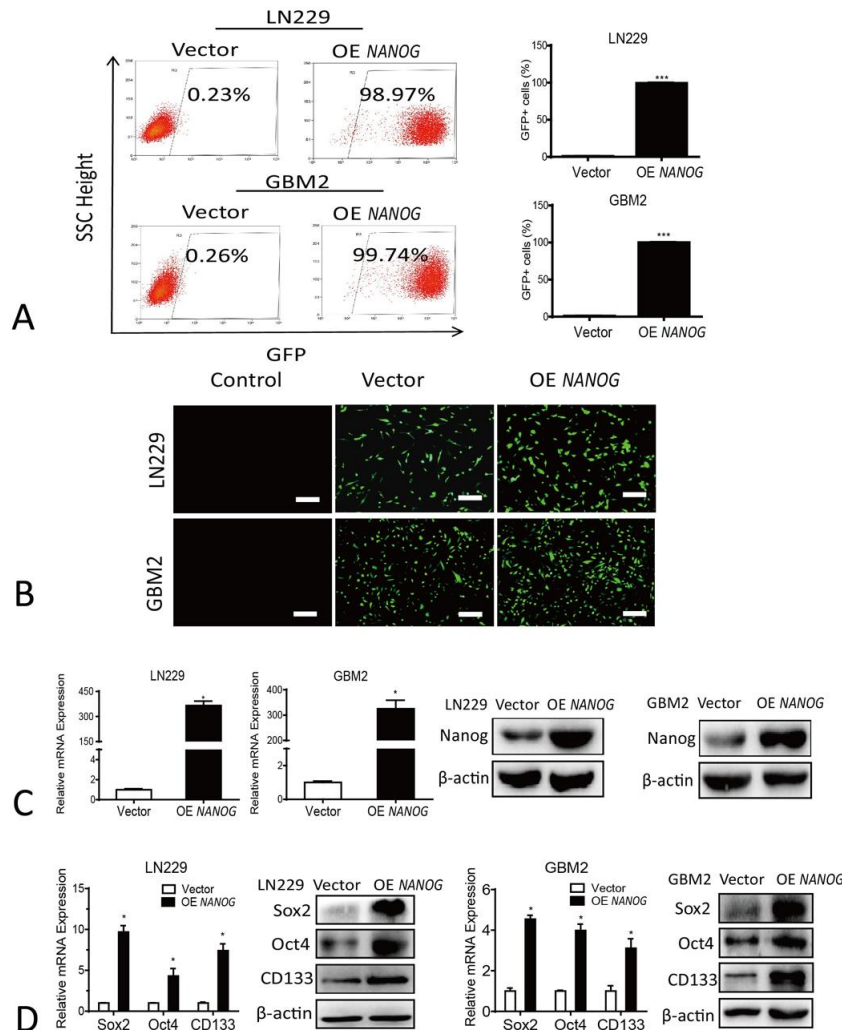
Figure 2. Overexpression of Nanog up-regulated cancer stem cells markers in established *NANOG* overexpression (OE *NANOG*) GBM cells. (A) GFP-positive GBM cells was testified by flow cytometry. (B) Representative images of GFP-positive LN229 and GBM2 cells and corresponding control cells. (scare bar=100 µm) (C) qRT-PCR and Western blot analysis confirmed the expression of Nanog in Nanog overexpressed LN229 and GBM2 cells and corresponding control cells. (D) qRT-PCR and Western blot analysis testified the expression of Sox2, Oct4 and CD133 in Nanog overexpressed LN229 and GBM2 cells and corresponding control cells. Data are means ± SD.*, *P* < 0.05. GFP, Green fluorescent protein.

increased in cells that were transduced to overexpress *NANOG* (Figure 2D).
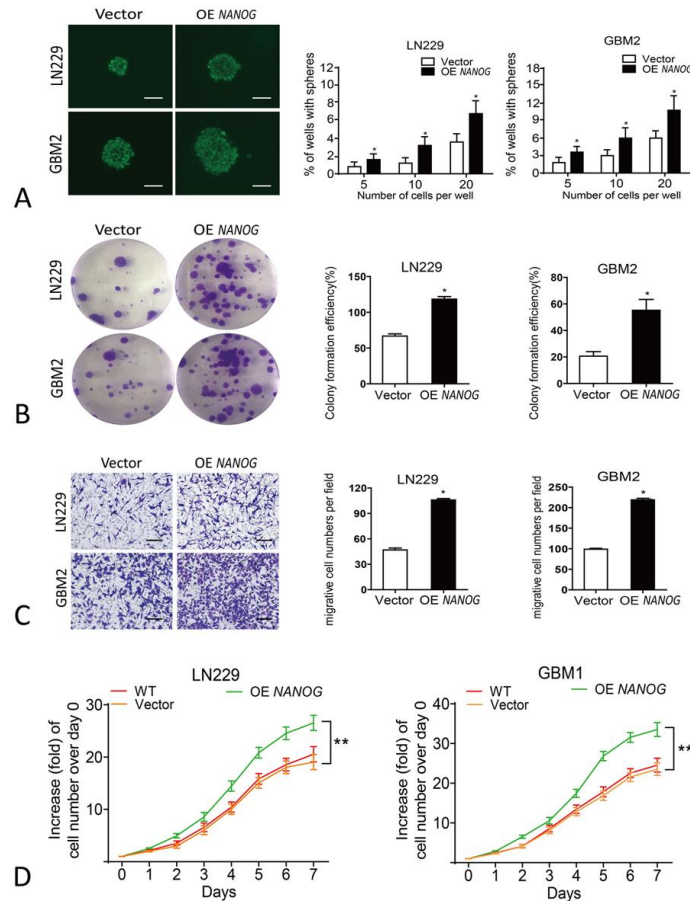
4.3. *NANOG* augments the stem-like traits and promotes formation of colonies, proliferation, and migration of GBM cells *in vitro*

Limiting dilution assays *in vitro* showed that overexpression of *NANOG* markedly enhanced the sphere-forming efficiency in GBM cells and increased their diameters (Figure 3A). CCK-8 assays showed that the size and quantity of colonies and proliferation rate were significantly increased in OE *NANOG* LN229 cells and GBM2 cells as compared with corresponding control and WT cells (Figure 3B,3D).

Emerging evidence has demonstrated that cancer stem cells (CSCs) play critical roles in tumor migration and recurrence. Transwell migration

Figure 3. Nanog augments the stem-like traits and promotes migration and invasion capabilities of GBM cells. (A) The size and efficiency of tumor-spheres formed by Nanog overexpressed LN229 and GBM2 and corresponding control cells.(scare bar=100μm) (B) Representative images of colony forming in Nanog overexpressed LN229 and GBM2 cells and corresponding control cells. (C) Representative images of Transwell migration assays in Nanog overexpressed LN229 and GBM2 cells and corresponding control cells. (scare bar=50μm)Data are means ± SD.*, $P < 0.05$.

assays demonstrated that overexpression of *NANOG* significantly increased the migratory (Figure 3C) capability of GBM cells.

4.4. Overexpression of *NANOG* activates the Hedgehog signaling pathway in GBM cells

NANOG has been identified as the downstream target for the Hedgehog signaling that plays crucial roles in tumor progression (15). Consistent with previous reports, analysis of Gravendeel GBM_database showed that expression of *NANOG* significantly correlated with expression of SMO and GLI1 (16) (Figure 4A). qRT-PCR and Western blot assays showed that overexpression of *NANOG* significantly increased the expression of Hedgehog signaling molecules, including Gli1, Gli2 and Smo (Figure 4B,4C). Existence of a positive feedback loop between NANOG and Hedgehog pathway was verified by dual-luciferase reporter system showing that *NANOG* increased the transcription of SMO and GLI1 in LN229 and GBM2 cells (Figure 4D, Figure 6) .

4.5. SANT-1 and GANT61 inhibit GBM progression

Smo and Gli1 are downstream regulators of the sonic hedgehog pathway. To assess the
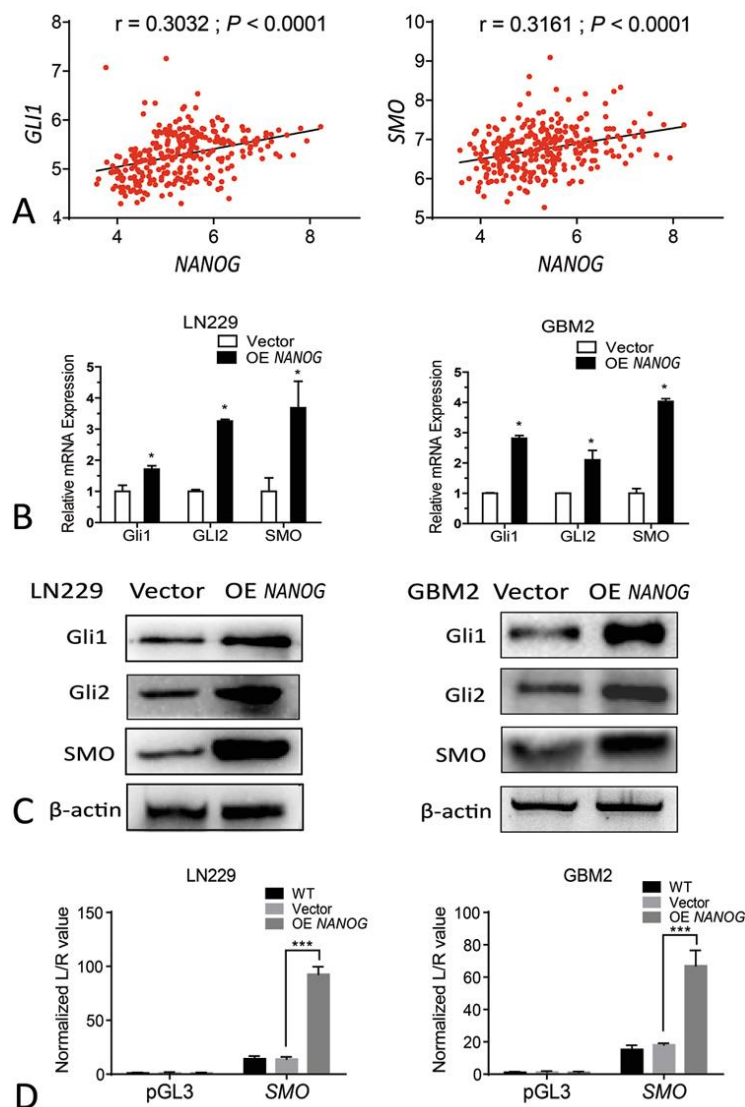
Figure 4. Overexpression of Nanog activates the SHH signaling pathway in GBM cells. (A) Pearson correlation analysis of *NANOG* and GLI1 expressions, *NANOG* and SMO expressions from Gravendeel database. (B) qRT-PCR analysis testified Gli1,Gli2 and SMO in Nanog overexpressed LN229 and GBM2 cells and corresponding control cells. (C) Western blot analysis testified Gli1, Gli2 and SMO in Nanog overexpressed LN229 and GBM2 cells and corresponding control cells. (D) Relative luciferase activities of reporter constructs containing the *NANOG* promoter in LN229 and GBM2 cells transfected with SMO expression plasmids compared that in empty vector-transfected (Vector) or untransfected (WT) (right panel) cells. Data are means ± SD.*, $P < 0.05$.

importance of targeting *NANOG* as a potential therapeutic target in GBM, we tested the potential of inhibiting SHH with combination of SANT-1, a high affinity antagonist of smoothened (SMO) and GANT61, a high affinity antagonist of Gli1. qRT-PCR assays showed that combination of SANT-1 and GANT61 antagonists significantly inhibited expression of Nanog as compared with control or treatment with

SANT-1 or GANT61 alone in LN229 and GBM2 cells indicating of the existence of a feedback loop (Figure 5A). CCK8 assay was carried out to assess the *in vitro* effect of SANT-1 and GANT61 in LN229 and GBM2 cells. Combination of SANT-1 and GANT61 antagonists significantly inhibited cell growth as compared with control or treatment with SANT-1 or GANT61 alone (Figure 5B).
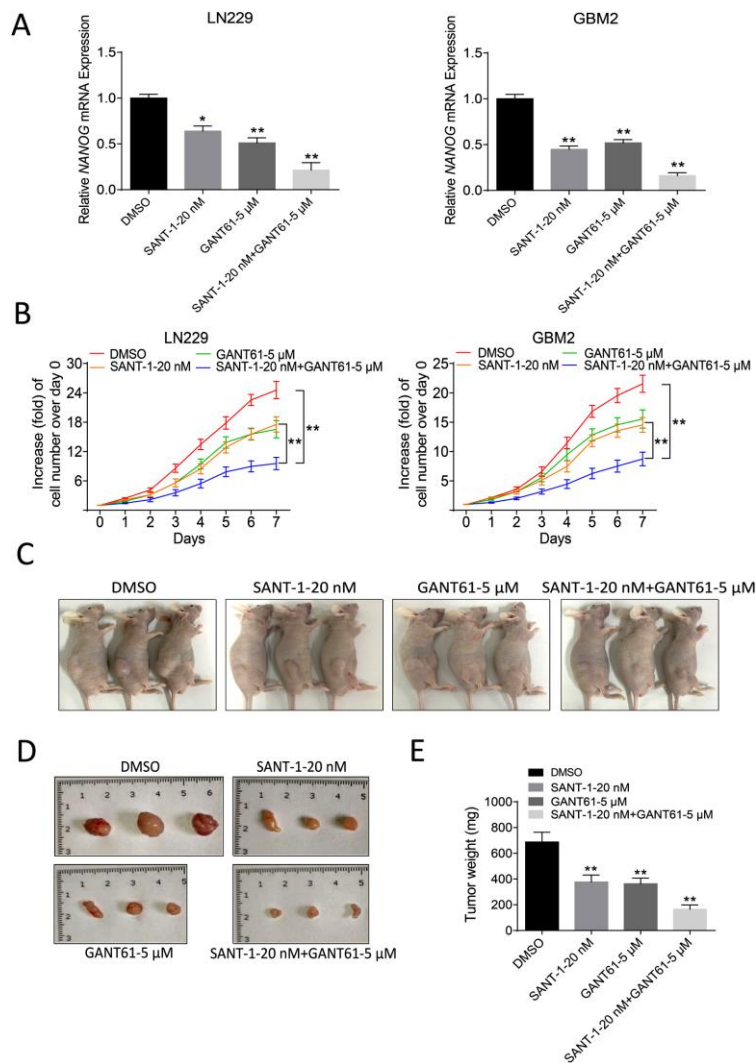
Figure 5. Combination therapy with SANT-1 and GANT61inhibits GBM progression. (A) qRT-PCR of Nanog in LN229 and GBM2 cells. (B) Cell proliferation curve of LN229 and GBM2 cells under different treatments testified by CCK-8 assay. (C) Tumor volume changes of different groups after the injection of LN229 cells. (D-E) comparison of dissected tumors of different groups 25 days after injection of HEI193 cells. Tumor weight of different groups 25 days after injection of LN229 cells. Data are means ± SD.*, $P < 0.05$, **, $P < 0.01$.

In addition, *in vivo* experiment revealed that the tumor size was significantly reduced in mice treated with SANT-1, or GANT61. However, the most striking reduction in tumor burden was achieved by treatment of mice with both SANT-1 and GANT61 (Figure 5C-E).

5. DISCUSSION

GBM is a tumor of glial cells or their precursors and is one of the most lethal human malignancies. These tumors are treated by surgical resection, radiotherapy plus adjuvant treatment with temozolomide (TMZ). Despite treatment, the survival of GBM patients remains less than 15 months (17, 18). Glioma stem cell-like cell (GSCL) which exhibit self-renewal and multi-directional differentiation are considered to be important to the generation, propagation, and resistance to chemoradiotherapy (19, 20).

Nanog and Hedgehog signaling pathway promote self-renewal of Embryonic stem cells
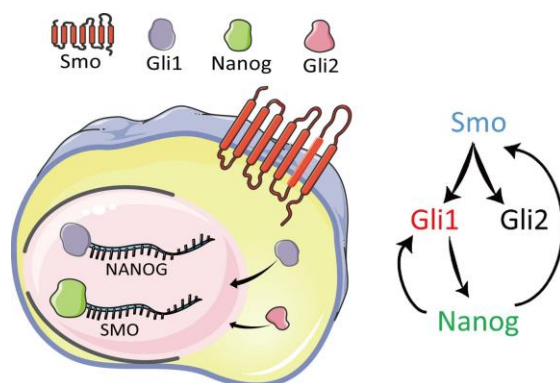
Figure 6. schematic diagram shows that Nanog not only serves as the down-stream of Hedgehog signaling through transcriptional activation by Gli1 but also increases the activity of Hedgehog signaling by activating Gli1and SMO in GBM cells.

(ESCs) and support progression of cancer. *NANOG*, play a critical role in maintaining self-renewal and pluripotency in normal embryonic stem cells, that has the potential to confer to cancer cells, stem-like traits including self-renewal and to enhance cell growth, reducing apoptosis and in enhancing tumorigenicity, metastasis, and drug-resistance in tumor cells by impacting NF-κB1 and JAK-STAT3 signaling pathway (21-25). The Hedgehog (HH) pathway is important in embryonic growth and development, and in directing cell fate (26). It has been shown that GSC expansion and specific expression of ESC-like stemness signature are dependent on the Hedgehog-Gli1 (HH-Gli1), which appears to exert its function through direct regulation of *NANOG*P8 (16). The direct regulatory interaction between Hedgehog signaling and Nanog is mediated by the Gli1 and Gli2, two downstream targets of Hedgehog that directly bind to the cis-regulatory sequence of the *NANOG* gene (27).

Here, we showed that stable *NANOG* overexpression in GBM cell lines by lentivirus system markedly increased CSC-associated genes in GBM cells and enhanced formation of tumor spheres, clone formation, and migration *in vitro*. We also showed that *NANOG* induced the signaling molecules of Hedgehog pathway suggesting of existence of a direct feedback loop between *NANOG* and this pathway. Existence of such a loop might be significant to the malignant behavior of GBM, making this loop as a possible therapeutic target. Nanog

augmented stem-like traits of GBM cells and activated SHH signaling pathway through a positive feedback loop that led to increase in Smo and Gli1.

Some inhibitors of SHH signaling pathway have been used in the treatment of non-small cell lung cancer (NSCLC), prostate cancer, glioma, and medulloblastoma (28-31). SANT-1, a high affinity antagonist of Smo, has induced apoptosis in a Ras/NFκB dependent manner in glioma and has reduced the tumor cell viability in pancreatic and prostate cancer cells (32). GANT61 which is a GLI inhibitor, has been reported to sensitizes glioma cells to the temozolomide treatment (33.) However, as yet, the combination of SANT-1 and GANT61 has not yet been tested in glioma cells (34). Here, we showed that use of inhibitors of Smo and Gli1 reduced tumor growth *in vivo*. Moreover, when combined together, the SANT-1 and GANT61 were more effective in decreasing the tumor burden. These findings suggest that the combination of these inhibitors might be useful in the treatment of GBM.

6. ACKNOWLEDGMENTS

7. REFERENCES

1. Brighi, C., Puttick, S., Rose, S. & Whittaker, A.K. The potential for remodelling the tumour vasculature in glioblastoma. Adv Drug Deliv Rev 136-137, 49-61 (2018)
DOI: 10.1016/j.addr.2018.10.001
PMid:30308226

2. Spence, M.I. & Lemberg, L. Ventricular tachycardia. Heart Lung 3, 657-661 (1974)

3. Schrub, J.C., Laumonier, R., Hillemand, B. & Clabaut, Y. [Esophago-gastric disorders in diabetes mellitus]. Sem Hop

45, 3161-3172 (1969)

4. Shi, Y., Guryanova, O.A., Zhou, W., Liu, C., Huang, Z., Fang, X., Wang, X., Chen, C., Wu, Q., He, Z., Wang, W., Zhang, W., Jiang, T., Liu, Q., Chen, Y., Wang, W., Wu, J., Kim, L., Gimple, R.C., Feng, H., Kung, H.F., Yu, J.S., Rich, J.N., Ping, Y.F., Bian, X.W. & Bao, S. Ibrutinib inactivates BMX-STAT3 in glioma stem cells to impair malignant growth and radioresistance. Sci Transl Med 10 (2018)
DOI: 10.1126/scitranslmed.aah6816
PMid:29848664 PMCid:PMC6431250

5. Levy, J.A. & Ziegler, J.L. Acquired immunodeficiency syndrome is an opportunistic infection and Kaposi's sarcoma results from secondary immune stimulation. Lancet 2, 78-81 (1983)
DOI: 10.1016/S0140-6736(83)90062-4

6. Geyer, G., Ebermann, R. & Barna, J. [Protein separation using polyacrylamide gel electrophoresis and demonstration of differences of the gamma-globulins in various diseases, rheumatism]. Z Rheumatol 33, 437-441 (1974)

7. Hopwood, J.J. & Elliott, H. Urinary excretion of sulphated N-acetyl-hexosamines in patients with various mucopolysaccharidoses. Biochem J 229, 579-586 (1985)
DOI: 10.1042/bj2290579
PMid:3931626 PMCid:PMC1145099

8. Seo, S., Jeon, H.Y. & Kim, H. Comparison of Cellular Transforming Activity of OCT4, NANOG, and SOX2 in Immortalized Astrocytes. DNA Cell Biol 36, 1000-1009 (2017)
DOI: 10.1089/dna.2017.3889
PMid:28933914

9. Yadav, P. & Shankar, B.S. Radio resistance in breast cancer cells is mediated through TGF-beta signalling, hybrid epithelial-mesenchymal pheno-type and cancer stem cells. Biomed Pharmacother 111, 119-130 (2018)
DOI: 10.1016/j.biopha.2018.12.055
PMid:30579251

10. Guo, L., Sun, C., Xu, S., Xu, Y., Dong, Q., Zhang, L., Li, W., Wang, X., Ying, G. & Guo, F. Knockdown of long non-coding RNA linc-ITGB1 inhibits cancer stemness and epithelial-mesenchymal transition by reducing the expression of Snail in non-small cell lung cancer. Thorac Cancer 10, 128-136 (2019)
DOI: 10.1111/1759-7714.12911
PMid:30485693 PMCid:PMC6360263

11. Wang, Z., Wang, B., Shi, Y., Xu, C., Xiao, H.L., Ma, L.N., Xu, S.L., Yang, L., Wang, Q.L., Dang, W.Q., Cui, W., Yu, S.C., Ping, Y.F., Cui, Y.H., Kung, H.F., Qian, C., Zhang, X. & Bian, X.W. Oncogenic miR-20a and miR-106a enhance the invasiveness of human glioma stem cells by directly targeting TIMP-2. Oncogene 34, 1407-1419 (2015)
DOI: 10.1038/onc.2014.75
PMid:24704830

12. Song, K., Yuan, Y., Lin, Y., Wang, Y.X., Zhou, J., Gai, Q.J., Zhang, L., Mao, M., Yao, X.X., Qin, Y., Lu, H.M., Zhang, X., Cui, Y.H., Bian, X.W., Zhang, X. & Wang, Y. ERBB3, IGF1R, and TGFBR2 expression correlate with PDGFR expression in glioblastoma and participate in PDGFR inhibitor resistance of glioblastoma cells. Am J Cancer Res 8, 792-809 (2018)

13. Yuan, Y., Yan, Z., Miao, J., Cai, R., Zhang, M., Wang, Y., Wang, L., Dang,

W., Wang, D., Xiang, D., Wang, Y., Zhang, P., Cui, Y., Bian, X. & Ma, Q. Autofluorescence of NADH is a new biomarker for sorting and characterizing cancer stem cells in human glioma. Stem Cell Res Ther 10, 330 (2019)
DOI: 10.1186/s13287-019-1467-7
PMid:31747975 PMCid:PMC6865050

14. Rota, L.M., Lazzarino, D.A., Ziegler, A.N., LeRoith, D. & Wood, T.L. Determining mammosphere-forming potential: application of the limiting dilution analysis. J Mammary Gland Biol Neoplasia 17, 119-123 (2012)
DOI: 10.1007/s10911-012-9258-0
PMid:22678420 PMCid:PMC3428520

15. Yao, P.J., Petralia, R.S. & Mattson, M.P. Sonic Hedgehog Signaling and Hippocampal Neuroplasticity. Trends Neurosci 39, 840-850 (2016)
DOI: 10.1016/j.tins.2016.10.001
PMid:27865563 PMCid:PMC5148655

16. Zbinden, M., Duquet, A., Lorente-Trigos, A., Ngwabyt, S.N., Borges, I. & Ruiz, I.A.A. NANOG regulates glioma stem cells and is essential *in vivo* acting in a cross-functional network with GLI1 and p53. EMBO J 29, 2659-2674 (2010)
DOI: 10.1038/emboj.2010.137
PMid:20581802 PMCid:PMC2928692

17. Pinel, S., Thomas, N., Boura, C. & Barberi-Heyob, M. Approaches to physical stimulation of metallic nanoparticles for glioblastoma treatment. Adv Drug Deliv Rev (2018)
DOI: 10.1016/j.addr.2018.10.013
PMid:30414495

18. Cloughesy, T.F., Cavenee, W.K. & Mischel, P.S. Glioblastoma: from molecular pathology to targeted treatment. Annu Rev Pathol 9, 1-25 (2014)
DOI: 10.1146/annurev-pathol-011110-130324
PMid:23937436

19. Laug, D., Glasgow, S.M. & Deneen, B. A glial blueprint for gliomagenesis. Nat Rev Neurosci 19, 393-403 (2018)
DOI: 10.1038/s41583-018-0014-3
PMid:29777182 PMCid:PMC6536307

20. Thomas, M.L. & Andress, M.R. Angioma of the knee demonstrated by angiography and arthrography. Report of a case. Acta Radiol Diagn (Stockh) 12, 217-220 (1972)
DOI: 10.1177/028418517201200211
PMid:5056028

21. Strauss, F.J. [Associations in change]. Freie Zahnarzt 18, 761-770, 793-800 (1974)

22. Lipkin, M. The hospital as a community facility: the medical staff and the hospital. Bull N Y Acad Med 48, 1396-1399 (1972)

23. Song, K., Chen, J., Ding, J., Xu, H., Xu, H. & Qin, Z. Hyperbaric oxygen suppresses stemness-associated properties and Nanog and oncostatin M expression, but upregulates beta-catenin in orthotopic glioma models. J Int Med Res, 1219672450 (2019)
DOI: 10.1177/0300060519872898
PMid:31813325

24. Huang, W., Zhong, Z., Luo, C., Xiao, Y., Li, L., Zhang, X., Yang, L., Xiao, K., Ning, Y., Chen, L., Liu, Q., Hu, X., Zhang, J., Ding, X. & Xiang, S. The miR-26a/AP-2alpha/Nanog signaling axis mediates stem cell self-renewal and temozolomide resistance in glioma. Theranostics 9, 5497-5516 (2019)
DOI: 10.7150/thno.33800

PMid:31534499 PMCid:PMC6735392

25. Zepecki, J.P., Snyder, K.M., Moreno, M.M., Fajardo, E., Fiser, A., Ness, J., Sarkar, A., Toms, S.A. & Tapinos, N. Regulation of human glioma cell migration, tumor growth, and stemness gene expression using a Lck targeted inhibitor. Oncogene 38, 1734-1750 (2019)
DOI: 10.1038/s41388-018-0546-z
PMid:30353164 PMCid:PMC6462869

26. Fink, D.M., Sun, M.R., Heyne, G.W., Everson, J.L., Chung, H.M., Park, S., Sheets, M.D. & Lipinski, R.J. Coordinated d-cyclin/Foxd1 activation drives mitogenic activity of the Sonic Hedgehog signaling pathway. Cell Signal 44, 1-9 (2018)
DOI: 10.1016/j.cellsig.2017.12.007
PMid:29284139 PMCid:PMC6503977

27. Pan, Q., Meng, L., Ye, J., Wei, X., Shang, Y., Tian, Y., He, Y., Peng, Z., Chen, L., Chen, W., Bian, X. & Wang, R. Transcriptional repression of miR-200 family members by Nanog in colon cancer cells induces epithelial-mesenchymal transition (EMT) Cancer Lett 392, 26-38 (2017)
DOI: 10.1016/j.canlet.2017.01.039
PMid:28163188

28. Giroux, L.E., Tolani, B., Li, H., Leguay, F., Hoang, N.T., Acevedo, L.A., Jin, J.Q., Tseng, H.H., Yue, D., Kim, I.J., Wislez, M., Wang, C., Jablons, D.M. & He, B. Membrane-bound full-length Sonic Hedgehog identifies cancer stem cells in human non-small cell lung cancer. Oncotarget 8, 103744-103757 (2017)
DOI: 10.18632/oncotarget.21781
PMid:29262597 PMCid:PMC5732763

29. Tong, W., Qiu, L., Qi, M., Liu, J., Hu, K.,

Lin, W., Huang, Y. & Fu, J. GANT-61 and GDC-0449 induce apoptosis of prostate cancer stem cells through a GLI-dependent mechanism. J Cell Biochem 119, 3641-3652 (2018)
DOI: 10.1002/jcb.26572
PMid:29231999

30. Yang, W., Liu, Y., Gao, R., Yu, H. & Sun, T. HDAC6 inhibition induces glioma stem cells differentiation and enhances cellular radiation sensitivity through the SHH/Gli1 signaling pathway. Cancer Lett 415, 164-176 (2018)
DOI: 10.1016/j.canlet.2017.12.005
PMid:29222038

31. Fuder, H., Buder, M., Riers, H.D. & Rothacher, G. On the opioid receptor subtype inhibiting the evoked release of 3H-noradrenaline from guinea-pig atria *in vitro*. Naunyn Schmiedebergs Arch Pharmacol 332, 148-155 (1986)
DOI: 10.1007/BF00511405
PMid:2871496

32. Li, J., Cai, J., Zhao, S., Yao, K., Sun, Y., Li, Y., Chen, L., Li, R., Zhai, X., Zhang, J. & Jiang, C. GANT61, a GLI inhibitor, sensitizes glioma cells to the temozolomide treatment. J Exp Clin Cancer Res 35, 184 (2016)
DOI: 10.1186/s13046-016-0463-3
PMid:27894350 PMCid:PMC5127098

33. Dixit, D., Ghildiyal, R., Anto, N.P., Ghosh, S., Sharma, V. & Sen, E. Guggulsterone sensitizes glioblastoma cells to Sonic hedgehog inhibitor SANT-1 induced apoptosis in a Ras/NFkappaB dependent manner. Cancer Lett 336, 347-358 (2013)
DOI: 10.1016/j.canlet.2013.03.025
PMid:23548480

34. Chenna, V., Hu, C. & Khan, S.R. Synthesis and cytotoxicity studies of

Hedgehog enzyme inhibitors SANT-1 and GANT-61 as anticancer agents. J Environ Sci Health A Tox Hazard Subst Environ Eng 49, 641-647 (2014)
DOI: 10.1080/10934529.2014.865425
PMid:24521409

Abbreviations: GBM:glioblastoma, ESCs:embryonic stem cells, CSCs:cancer stem-like cells, GEO:Gene Expression Omnibus, KEGG:Kyoto Encyclopedia of Genes and Genomes, GSEA:Gene Set Enrichment Analysis, GO:Gene Ontology, WT:wild type, Smo: Smoothened, Frizzled Class Receptor, Gli1:GLI Family Zinc Finger 1, GFP:green fluorescent protein, SD:Standard Deviation, SOX2:SRY-Box Transcription Factor 2, OCT4:Octamer-Binding Protein 4

Send correspondence to: Deyu Guo, Institute of Pathology and Southwest Cancer Center, Southwest Hospital, Third Military Medical University (Army Medical University), and Key Laboratory of Tumor Immunopathology, Military of Education of China, Chongqing, China, Tel:18083010689, E-mail: 2580685422@qq.com